Overexpression of integrin β_2 improves migration and engraftment of adipose-derived stem cells and augments angiogenesis in myocardial infarction

Zihui Yuan[1], Kai Yan[1,2], Jian Wang[1]

[1]Department of Vascular Surgery, Union Hospital, Tongji Medical College, Huazhong University of Science and Technology, Wuhan, China; [2]Department of Hepatobiliary and Gastrointestinal Surgery, Hankou Hospital, Wuhan, China

Contributions: (I) Conception and design: J Wang; (VII) Administrative support: J Wang; (III) Provision of study material or patients: Z Yuan, K Yan; (IV) Collection and assembly of data: Z Yuan; (V) Data analysis and interpretation: Z Yuan, K Yan; (VI) Manuscript writing: All authors; (VII) Final approval of manuscript: All authors.

Correspondence to: Jian Wang, MD, PhD. Department of Vascular Surgery, Union Hospital, Tongji Medical College, Huazhong University of Science and Technology, 1277 Jiefang Avenue, Wuhan 430022, China. Email: Jianwang1030@126.com.

Background: Adipose-derived stem cells (ASCs) hold a great promise for myocardial infarction, but therapeutic efficacy appears to be limited by their poor survival and engraftment. Integrins are transmembrane proteins known to regulate the biological behaviors of stem cells. Integrin β_2 (ITGB2) specifically binds to intercellular cell adhesion molecule-1 (ICAM-1), which is upregulated in infarcted myocardium. ASCs typically express an insufficient amount of ITGB2, and this may limit their homing and engraftment abilities.

Methods: ASCs were lentivirally transduced to overexpress ITGB2. ITGB2 messenger RNA (mRNA) and protein expression were examined by quantitative polymerase chain reaction (PCR) and western blot. Cell viability, proliferation, and migration were assessed *in vitro*. Adipogenic and osteogenic differentiation were induced, and the mRNA expressions of specific differentiation markers were quantified by PCR. ICAM-1 expression in the infarcted myocardium was quantified at 3 and 7 days after myocardial infarction. ITGB2-transfected ASCs (ITGB2-ASCs), control ASCs (CTRL-ASCs), and phosphate-buffered saline (PBS) were intramyocardially injected into the peri-infarct region at 3 days after coronary ligation. Four weeks after transplantation, myocardial blood perfusion was measured by $^{13}N{\cdot}NH_3{\cdot}H_2O_2$ positron emission tomography (PET)/computed tomography (CT). Explanted hearts were then processed for the measurement of capillary density, the quantification of survived green fluorescent protein (GFP^+) ASCs, and the identification of ASCs coexpressing angiogenic growth factors.

Results: ICAM-1 expression peaked at 3 days after myocardial infarction and remained elevated over the remote normal myocardium at 7 days after myocardial infarction. ITGB2-ASCs displayed a significant increase in cell viability, proliferation rate, and migration index when compared with CTRL-ASCs. Adipogenic and osteogenic differentiation were more enhanced in ITGB2-ASCs than in CTRL-ASCs. Four weeks after transplantation, surviving GFP^+ ASCs were significantly increased, ASCs expressing angiogenic growth factors were more pronounced, capillary density was substantially enlarged, and myocardial blood perfusion was markedly improved in the hearts that received ITGB2-ASCs implantation when compared to those that underwent CTRL-ASC treatment.

Conclusions: ITGB2 overexpression of ASCs enhanced cell viability, proliferation, and migration and induced differentiation *in vitro*. ITGB2 overexpression significantly improved the survival and engraftment of ASCs into infarcted myocardium via ITGB2/ICAM-1 interaction, augmented angiogenesis, and ultimately improved blood perfusion in infarcted myocardium.

Keywords: Integrin; adipose-derived stem cells; myocardial infarction; positron emission computed tomography

Submitted Jun 09, 2022. Accepted for publication Jul 25, 2022.
doi: 10.21037/atm-22-3339
View this article at: https://dx.doi.org/10.21037/atm-22-3339

Introduction

Adipose-derived stem cells (ASCs) from the stromal-vascular fraction of adipose tissues have shown great potential in stem cell-based treatment of injured myocardium. These cells are available in sufficient quantities, can be easily harvested, possess multipotent capabilities, and proliferate rapidly (1,2). ASCs are capable of differentiating into endothelial cells (3,4) and smooth muscle cells (5,6) and participating in vessel formation. Importantly, ASCs secrete multiple proangiogenic growth factors, such as vascular endothelial growth factor (VEGF) and hepatocyte growth factor (HGF), at levels that are bioactive (7-9).

Despite the potential advantages of ASCs, low therapeutic efficacy due to poor cell survival and extensive redistribution throughout the body remains a significant obstacle in stem cell therapy. The deprivation of oxygen and nutrient supply and the inflammatory microenvironment in the ischemic myocardium cause massive cell apoptosis and death within a few days after transplantation of cells into ischemic myocardium (10-12). Within 2 to 6 days of delivery, the majority of transplanted cells migrate and redistribute to extracardiac organs through the myocardial venous and lymphatic systems (13-15). Studies have shown that the implantation of ASCs results in an approximately 5% increase in ejection fraction (16-19), and this moderate improvement is far from satisfactory.

Integrins, heterodimeric transmembrane proteins composed of α and β subunits, are implicated in cell-to-extracellular matrix (ECM) adhesion (20). Integrins transmit ECM cues to the intracellular signaling pathway, and ECM-integrin signaling regulates various cellular functions such as cell viability, proliferation, migration, and differentiation (21). Apoptosis occurs upon cell detachment from ECM. Integrins are the vital cell-surface receptor for cell-ECM interaction, and they suppress cell apoptosis and resolve the poor survival of implanted cells (22,23). Intercellular cell adhesion molecule-1 (ICAM-1), the ligand for integrin β_2 (ITGB2), is upregulated by muscular ischemia in endothelial cells (24). Endothelial progenitor cells expressing ITGB2 attach to endothelial cells specifically through ITGB2/IACM-1 interaction (24). ASCs typically express insufficient ITGB2, which limits their homing, engraftment, and survival after transplantation (25,26). We genetically modified ASCs to overexpress ITGB2 with the intention to enhance adhesion and ultimately cell survival after implantation. ITGB2-overexpressing ASCs (ITGB2-ASCs) efficiently engraft into infarcted myocardium as they abundantly express ICAM-1, the ligand for ITGB2. Therefore, the implantation of ITGB2-ASCs could be expected to amplify benefit effects on myocardial infarction.

The purpose of this study was to address the following questions: (I) whether myocardial ischemia selectively increases the expression of ICAM-1, which specifically interacts with ITGB2; (II) whether overexpression of ITGB2 on ASCs enhances cell viability, proliferation, migration, and differentiation; (III) whether overexpression of ITGB2 on ASCs promotes homing and engraftment to ischemic myocardium through ITGB2/ICAM-1 banding; (IV) whether implantation of ITGB2-ASCs eventually augments angiogenesis and improves blood perfusion in infarcted myocardium. We present the following article in accordance with the ARRIVE reporting checklist (available at https://atm.amegroups.com/article/view/10.21037/atm-22-3339/rc).

Methods

The animal experiments were approved by the Institutional Animal Ethical Committee (IAEC) of Huazhong University of Science and Technology (No. 2017-392), in compliance with the institutional guidelines for the care and use of animals. A protocol was prepared without registration before the study.

Isolation and culture of ASCs

ASCs were isolated from male green fluorescent protein (GFP) transgenic rats. Abdominal subcutaneous and inguinal adipose tissue were collected, minced, and digested with 0.2% collagenase I (Worthington Biochemical Corporation, Lakewood, NJ, USA) at 37 ℃ for 20–30 minutes. Collagenase activity was inactivated by adding Dulbecco's Modified Eagle Medium F12 (DMEM-F12; HyClone, Logan, UT, USA) containing 15% fetal bovine serum (FBS). The digested adipose tissue was filtered twice with a 100 μm

and then with a 25 μm nylon membrane to eliminate the undigested fragments. Cellular suspension was centrifuged at 300 ×g for 5 minutes. The supernatant was discarded, and cell pellets were resuspended in cell culture medium (CCM) and cultivated for 24 hours at 37 ℃ in 5% CO_2.

Lentiviral vector construction and transduction of ITGB2

The nucleotide sequence coding for the ITGB2 was cloned into the lentiviral vector. The empty vector was utilized as a negative control. 293T cells were transiently transfected using lipofectamine 2000 to produce lentiviral vector particles carrying a ITGB2 transgene. The day before transfection, a total of 4×10^6 293FT cells were plated on 10 cm tissue culture dishes and reached approximately 70% confluence at the time of transfection. The three-plasmid recombinant lentiviral vector system mainly comprised packaging plasmid (20 μg), envelope plasmid (10 μg), and vector plasmid (20 μg). The supernatant was harvested 48 hours later. The supernatant containing viral particles was centrifuged at 5,000 ×g for 30 minutes and passed through a 0.45 μm cellulose acetate filter to remove cell debris. Subsequently, the separated viral particles were concentrated by polyethylene glycol precipitation. The virus particles were resuspended in phosphate-buffered saline (PBS), aliquoted, and stored at –80 ℃.

Cells were stably infected with the lentiviral vector carrying the ITGB2 genes at a high multiplicity of infection (MOI) of 50 in the presence of 8 μg/mL polybrene. The lentiviral vector introduced ITGB2 plasmid DNA into the ASCs' genome. One day prior to lentiviral transduction, cells were plated on 10 cm culture dishes and reached 60–70% confluence. Then, the cells were incubated in CCM containing the empty or viral vector for 48 hours. The viral infection of ASCs was confirmed by quantitative polymerase chain reaction (PCR) and western blotting for the expression of ITGB2 messenger RNA (mRNA) and protein.

MTT assay

Cell viability was determined using a 3-(4,5-dimethylthiazol-2-yl)-2,5-diphenyl tetrazolium bromide (MTT) assay (Sigma-Aldrich, St Louis, MO, USA). ASCs were plated in 96-well plates at a density of 1×10^3 cells per well and cultured for 12 hours. After washing 3 time using PBS, MTT was added to each well at a final concentration of 0.5 mg/mL, and the cells were incubated for 4 hours at 37 ℃ for MTT-formazan formation. The supernatant was discarded, and 100 μL of dimethyl sulfoxide (DMSO) was added into each well for 5 minutes at room temperature. The absorbance at 570 nm was recorded in a 96-well microplate reader.

Cell proliferation assays

Cell proliferation was determined using a Cell Counting Kit-8 (CCK-8; Dojindo, Kumamoto, Japan) assay according to the manufacturer's instructions. Briefly, ASCs were seeded in 96-well plates (3×10^3 cells/well) and examined at 24 hours. The detection buffer (100 μL, ratio of medium to CCK-8 was 9:1) was added to each well. After incubation for 2 hours at 37 ℃, the absorbance at 450 nm was detected by a SpectraMax M5 multi-mode microplate reader (Molecular Devices, San Jose, CA, USA).

Transwell assay

Cell migration assay was performed with 8 μm pore size transwell cell culture chambers. Cell suspension (5×10^5 cells/mL) was loaded into the upper chamber, while DMEM supplemented with 10% FBS containing SDF-1α was added into the lower chamber. The chamber was incubated at 37 ℃ for 24 hours. Cells that had migrated to the lower surface of the chamber membrane were fixed for 5 minutes in 100% methanol and stained with 0.1% crystal violet for 2 minutes. The cells on the upper surface of the membrane were removed with cotton swabs. After 3 washes with PBS, the number of migrated cells were counted under an inverted microscope.

Adipogenic differentiation and Oil Red O staining

Adipogenic differentiation was induced by culturing the cells for 12 days in DMEM containing 5% FBS, 10 μM bovine insulin, 250 isobutyl-methylxanthine, 200 μM indomethacin, 1 μM dexamethasone, 5 μg/mL streptomycin, and 5 U/mL penicillin. Intracellular lipid accumulation was observed by Oil Red O staining. The cells were fixed in 4% paraformaldehyde for 30 minutes at room temperature and then stained with Oil Red O reagent (0.5% in isopropanol) for 15 minutes. The excess stain was removed by isopropanol incubation for 15 minutes at room temperature and repeated washing in distilled water. The lipid droplets in the cells stained with Oil Red O and were observed under microscope. Oil Red O staining of cells was determined by measuring the optical density at 495 nm with a spectrophotometer.

Table 1 Primer sequences for quantitative RT-PCR

Gene	Primers
ITGB2	
Sense	5'-AATGGACCCCAAGAGCTTTG-3'
Antisense	5'- TCGGAAAGTCACATTGAATGC-3'
LPL	
Sense	5'-GTGAGAACATTCCCTTCACCCT-3'
Antisense	5'-CCAGCGGAAGTAGGAGTCGT-3'
PPAR-γ	
Sense	5'-CCTTTACCACGGTTGATTTCTC-3'
Antisense	5'-CAGGCTCTACTTTGATCGCACT-3'
BSP	
Sense	5'-AGCTGACGCTGGAAAGTTGG-3'
Antisense	5'-TCAGTGACGCTTGCCTCCTC-3'
Osterix	
Sense	5'-TCAAGCACCAATGGACTCCTC-3'
Antisense	5'-TATCCAAGGACGTGTAGACACTAGG-3'
GAPDH	
Sense	5'-GCCAAGGTCATCCATGACAAC-3'
Antisense	5'-GTGGATGCAGGGATGATGTTC-3'

RT-PCR, reverse transcription polymerase chain reaction; ITGB2, integrin β_2; LPL, lipoprotein lipase; PPAR-γ, peroxisome proliferator-activated receptors-γ; BSP, bone sialoprotein; GAPDH, glyceraldehyde-3-phosphate dehydrogenase.

Osteogenic differentiation and alkaline phosphatase staining

Osteogenic induction was carried out by cultivating the cells for 28 days in DMEM containing 10% FBS, 10 mM β-glycerophosphate, 50 μM ascorbate-2-phosphate, 10 nm $1,25(OH)_2$ vitamin D_3, 5 μg/mL streptomycin, and 5 U/mL penicillin. ECM calcification was examined by alkaline phosphatase staining. After fixation with 4% paraformaldehyde for 30 minutes at room temperature and washing twice with distilled water, the cells were incubated in alkaline phosphatase detection buffer containing nitro blue tetrazolium (NBT) and 5-Bromo-4-chloro-3-indolyl phosphate (BCIP) for 30 minutes at 37 ℃. Alkaline phosphatase catalyzed and hydrolyzed the substrate of BCIP to form an immediate product, which reacted with the NBT and produced an insoluble brown dye. Stained cells were then observed under a light microscope. The brown product was also quantified by reading the absorbance in a microplate spectrophotometer at a wavelength of 465 nm.

Quantitative PCR

Total RNA was extracted from ASCs using TRI Reagent (Sigma-Aldrich). The concentration of total RNA was detected and quantified using a biological spectrometer. Complementary DNA (cDNA) was synthesized from 1 μg of total RNA with a reverse transcriptase 1st-Strand cDNA Synthesis System kit (Invitrogen, Waltham, MA, USA). The synthesized cDNA was subjected to quantitative real-time PCR reaction with the help of a StepOne™ Real-Time PCR System (Applied Biosystems, Foster City, CA, USA). GAPDH was used as an internal reference. The genes for ITGB2, the adipogenic differentiation markers lipoprotein lipase (LPL) and peroxisome proliferator-activated receptor gamma (PPAR-γ), and the osteogenic differentiation markers bone sialoprotein (BSP) and osterix (OSX) were analyzed. Primer sequences for this experiment are shown in *Table 1*. All reactions were conducted in triplicate.

Western blot analysis

ASCs were lysed on ice with a radioimmunoprecipitation assay buffer (RIPA) buffer protease inhibitor cocktail (Roche, Basel, Switzerland) and a phosphate inhibitor (Sigma-Aldrich). After humanely sacrificing the animals, the hearts were removed and kept in liquid nitrogen until analysis. The heart samples were homogenized, and the lysates were sonicated for 10 seconds and centrifuged at 12,000 rpm for 15 minutes. Protein concentrations were determined spectrophotometrically using a Pierce BCA Protein Assay Kit (Thermo Fisher Scientific, Rockford, IL, USA). The protein samples were separated by 10% or 15% dodecylsulphate polyacrylamide gel electrophoresis (SDS-PAGE) gels, transferred to polyvinylidene difluoride (PVDF) membranes and blocked with Tris-buffered saline containing 0.05% Tween-20 (TBST) and 5% non-fat milk powder for 2 hours. The membranes for the cell lysates were incubated with primary anti-ITGB2 mouse polyclonal antibody (Cell signaling Technology, Beverly, MA, USA). The membranes for the tissue lysates were incubated with primary mouse anti-ICAM-1 polyclonal antibodies (Proteintech, Chicago, IL, USA) overnight at 4 ℃. Equal loading of all lanes was confirmed by reprobing the membrane with anti-glyceraldehyde 3-phosphate dehydrogenase (GAPDH) mouse monoclonal antibodies

(Proteintech) overnight at 4 ℃. After 5 washes with TBST, the membranes were incubated with horseradish peroxidase (HRP)-conjugated anti-mouse secondary antibodies (Pierce, Rockford, IL, USA) for 1 hour at room temperature. The protein samples were visualized using a chemiluminescence method. The intensities of the specific western blot bands were quantified using the Software ImageJ (National Institutes of Health, Bethesda, MD, USA) and normalized against GAPDH.

Immunofluorescent staining

Adherent ASCs, grown in chamber slides, were fixed using 4% cold paraformaldehyde at 4 ℃ for 20 minutes, followed by permeabilization with cold methanol (–20 ℃) for 5 minutes. Subsequently, the cells were incubated with an anti-ITGB2 rabbit polyclonal antibody (Cell signaling Technology) at 4 ℃ overnight. Next, the cells were incubated with an Alexa Fluor 594 conjugated donkey anti-rabbit IgG secondary antibody (Thermo Fisher Scientific) at room temperature for 1 hour. Finally, the cells were visualized using a confocal fluorescence microscope (Olympus Corp., Tokyo, Japan).

Hearts were then sliced coronally into 10-μm-thick sections at –20 ℃ on a cryotome. Tissue sections were fixed in cold methanol for 5 minutes, incubated in PBS with 0.1% Trton-X-100 for 15 minutes, and then blocked with 5% bovine serum albumin (BSA) for 30 minutes at room temperature. Finally, the slides were incubated with primary antibodies for 1 hour at 37 ℃. ICAM-1, the ligand for ITGB2, was detected by an anti-ICAM-1 rabbit polyclonal antibody (Santa Cruz Biotechnology, Santa Cruz, CA, USA). von Willebrand factor (VWF), an endothelial cell marker, was identified by a rabbit anti-VWF antibody (Santa Cruz Biotechnology). After 3 more washes with PBS, the slides were incubated with Alexa Fluor 594 conjugated donkey anti-rabbit IgG for 45 minutes at 37 ℃. After 3 more washes with PBS, the slides were stained for nuclei using 4',6-diamidino-2-phenylindole (DAPI). Images of sections were obtained by a confocal fluorescence microscope (Olympus Corp.).

Myocardial infarction model

Female inbred Lewis rats (n=24, 6 weeks old, 180–200 g) were provided by the Experimental Animal Center of Wuhan University (Wuhan, China). Rats were intubated, anaesthetized with oxygen/isoflurane, and mechanically ventilated. A left anterior thoracotomy was performed, the heart was exposed, and the left anterior descending artery (LAD) was permanently occluded at about 2–3 mm from its origin using a 7-0 silk suture. Infarction was confirmed by myocardial blanching. Sham surgery involved the same cardiac exposure without placement of the coronary suture. At 3 and 7 days following coronary occlusion, 6 rats (n=3 per time-point) were euthanized, and the hearts were carefully removed for the identification of ICAM-1.

Three days after LAD occlusion, the rats were randomly assigned to 3 groups (PBS, n=6; CTRL-ASCs, n=6; and ITGB2-ASCs, n=6). We selected a medium sample size (n=6) to produce conclusive results and avoid unnecessary use of animals. In 2 ASC treatment groups, 150 μL of 1.5×10^6 GFP-positive ASCs were intramyocardially injected into 4 to 6 sites in the peri-infarct zone. PBS control rats underwent the injection of 150 μL PBS in the same regions. Four weeks after cell transplantation, the rats were subjected to positron emission tomography (PET)/computed tomography (CT) examination. The rats were then euthanized, and the hearts were harvested for histological analysis. The researchers who were responsible for the outcome assessment and data analysis were not aware of the group allocation and the conduct of the experiment.

PET/CT imaging

All PET/CT scans were performed on a small animal PET/CT scanner 4 weeks post-transplantation. Rats were anesthetized with inhaled 2% isoflurane and placed on a scanning table. Then, the rats were injected with approximately 500±25 μCi of ^{13}N-ammonia (^{13}N-$NH_3\cdot H_2O$) through the tail vein. Cardiac PET/CT scans were performed immediately with the 10-minute dynamic acquisition mode, followed by CT images in static mode on the TransPET Discoverist 180 system (Raylan Technology Co., Ltd, Suzhou, China). The PET images were reconstructed iteratively using the three-dimensional (3D) ordered subset expectation maximization (OSEM) method. CT images were reconstructed using the Feldkamp algorithm. Images were analyzed using Carimas 2 software (Turku PET Center, Turku, Finland). ^{13}N-$NH_3\cdot H_2O$ uptake was calculated as the standardized uptake value (SUV) based on the following formula: the mean pixel value with the decay-corrected region-of-interest activity (μCi/kg) was divided by injected dose (μCi) and body weight (kg). The value of the left ventricular (LV) segment with the maximum SUV was set as 100%, and the values of other

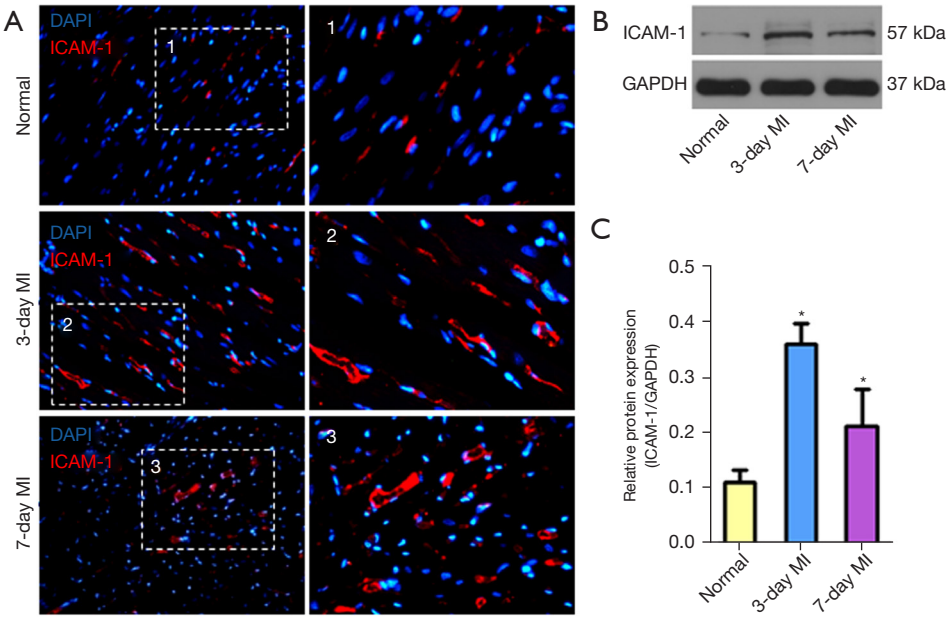

Figure 1 Overexpression of ICAM-1 in infarcted myocardium. (A) Immunofluorescent staining indicated that ICAM-1 was present in infarcted tissue and blood vessels at 3 and 7 days after myocardial infarction. (B,C) Relative expression of ICAM-1 protein in infarcted myocardium peaked at 3 days and remained elevated at 7 days after MI. Scale bar: 50 μm. *P<0.05 versus remote normal myocardium. ICAM-1, intercellular cell adhesion molecule-1; MI, myocardial infarction; GAPDH, glyceraldehyde-3-phosphate dehydrogenase.

segments were normalized according to the maximum SUV.

Statistical analysis

All statistical analyses were performed using SPSS software (IBM Corp., Armonk, NY, USA). Continuous variables were expressed as the mean ± standard deviation with normal distribution. Comparisons between 3 groups were made using a two-tailed Student's *t*-test. Comparisons among multiple groups were made using two-way analysis of variance (ANOVA). A P value of <0.05 was considered statistically significant.

Results

Myocardial infarction increased expression of ICAM-1 in infracted myocardium

Immunofluorescence examination showed that ICAM-1 was highly expressed in both cardiomyocytes and blood vessels in infracted myocardium at 3 and 7 days following myocardial infarction, in contrast to the remote normal myocardium (*Figure 1A*). Western blotting showed that the relative expression level of ICAM-1 protein (normalized to GAPDH) peaked at 3 days after myocardial infarction (0.36±0.04) and remained elevated at 7 days after myocardial infarction (0.21±0.07) over the baseline in normal myocardium (0.11±0.02; *Figure 1B,1C*).

Genetically modified ASCs highly expressed ITGB2, the ligand of ICAM-1

Immunofluorescent staining revealed that ASCs transfected with lentivirus vector containing ITGB2 genes (ITGB2-ASCs) robustly expressed ITGB2, which indicated that these cells have the potential to attach to endothelial cells through ICAM-1/ITGB2 interaction (*Figure 2A*). Quantitative PCR indicated that the relative expression of ITGB2 mRNA (normalized to GAPDH) was significantly higher in ITGB2-ASCs (1.11±0.12) than in CTRL-ASCs (0.52±0.09; *Figure 2B*). Western blotting revealed a significantly stronger expression of ITGB2 protein (normalized to GAPDH) with molecular weights of 84 kDa in ITGB2-ASCs (0.75±0.04) than in CTRL-ASCs (0.48±0.02; *Figure 2C,2D*).

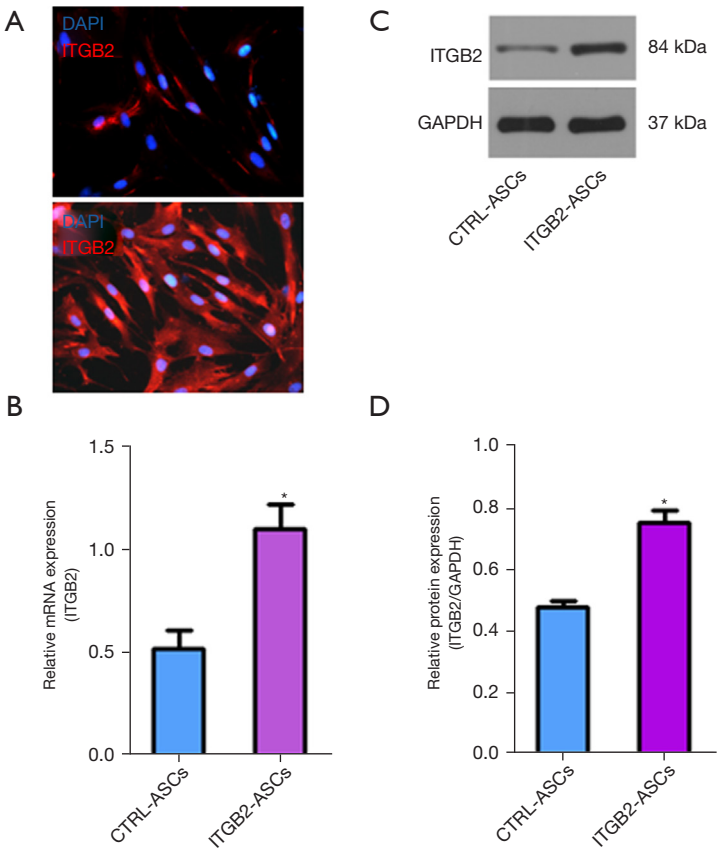

Figure 2 High expression of ITGB2 in genetically modified ASCs. (A) Immunofluorescent staining revealed that ASCs were transfected with ITGB2-harboring lentivirus and expressed ITGB2. (B) Quantitative PCR indicated that mRNA levels of ITGB2 were significantly higher in ITGB2-ASCs than in CTRL-ASCs. (C,D) Western blotting showed that the expression of ITGB2 with 84kDa was more increased in ITGB2-ASCs than in CTRL-ASCs. Scale bar: 50 μm. *P<0.05 versus CTRL-ASCs. ASCs, adipose-derived stem cells; ITGB2, integrin β_2; GAPDH, glyceraldehyde-3-phosphate dehydrogenase; PCR, polymerase chain reaction; CTRL, control; mRNA, messenger RNA; DAPI, 4',6-diamidino-2-phenylindole.

ITGB2 overexpression of ASCs enhanced viability, proliferation, and migration

Cell viability evaluated by MTT assay was statistically higher in ITGB2-ASCs (89.33%±2.28%) than in CTRL-ASCs (74.41%±6.72%; *Figure 3A*). Cell proliferation percentage reflected by CCK-8 assay was obviously greater in ITGB2-ASCs (125.78%±6.58%) than in CTRL-ASCs (97.82%±4.93%; *Figure 3A*). Boyden chamber assay revealed a higher density of ITGB2-ASCs than CTRL-ASCs in the presence of 50 ng and 100 ng of SDF-1α (*Figure 3B*). Migration index was significantly more increased in ITGB2-ASCs than in CTRL-ASCs under the stimulation of 50 ng of SDF-1α (55.00±3.58 *vs.* 41.00±4.60) and 100 ng of SDF-1α (76.83±4.36 *vs.* 48.00±4.60; *Figure 3C*).

ITGB2 overexpression of ASCs promoted induced differentiation

Oil Red O staining indicated the accumulation of oil droplets in ASCs that differentiated to adipocytes (*Figure 4A*). The expression of the adipogenic-related genes LPL and PPAR-γ mRNA (normalized to GAPDH) was significantly higher in ITGB2-ASCs than in CTRL-ASCs after 12-day adipogenic induction (1.15±0.02 *vs.* 0.54±0.10 for LPL and 1.22±0.11 *vs.* 0.46±0.14 for PPAR-γ; *Figure 4B*). Osteogenic differentiation potential was determined by alkaline phosphatase staining (*Figure 4C*). Following 28-day osteogenic induction, ITGB2-ASCs exhibited a significantly higher expression of osteogenic-related genes BSP and OSX mRNA (normalized to GAPDH) when compared to CTRL-ASCs (1.01±0.13

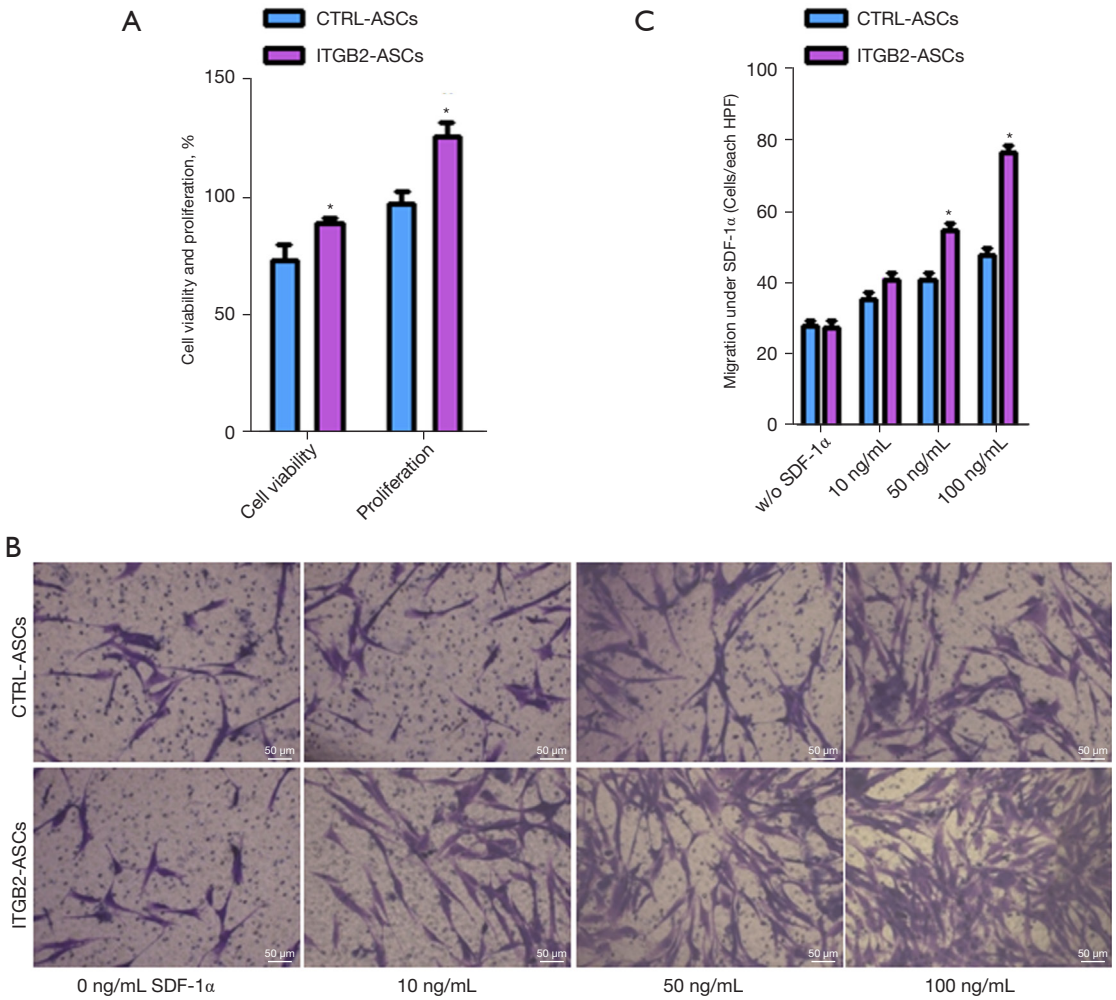

Figure 3 Enhancement of ASC viability, proliferation, and migration by ITGB2 overexpression in vitro. (A) Viability and proliferation of ITGB2-ASCs were significantly greater than those of CTRL-ASCs. (B,C) The migration of ITGB2-ASCs was enhanced in the presence of 50-ng and 100-ng SDF-1α. The cells on the lower surface of the membrane were stained with crystal violet. Scale bar: 50 μm. *P<0.05 versus CTRL-ASCs. ASCs, adipose-derived stem cells; ITGB2, integrin β_2; CTRL, control; SDF-1α, stromal cell derived factor-1 alpha; HPF, high power field.

vs. 0.49±0.02 for BSP and 1.16±0.07 *vs.* 0.46±0.18 for OSX; *Figure 4D*).

ITGB2 overexpression of ASCs improved the engraftment in infracted myocardium post-transplantation

Injected ASCs were tracked by microscopic detection of GFP. At 4 weeks after cell implantation, CTRL-ASCs and ITGB2-ASCs were detected in all 6 hearts from the cell-treated groups, suggesting successful engraftment and survival of the injected ASCs (*Figure 5A-5C*). Importantly, more GFP-positive ASCs were evident in the hearts that received ITGB2-ASC implantation than in the hearts that underwent CTRL-ASC treatment. The numbers of survived and engrafted ASCs, quantified as GFP-positive cells per high-power field (HPF), was significantly greater in the hearts that received ITGB2-ASC implantation (36.33±7.12 cells per HPF) than in the hearts that underwent CTRL-ASC treatment (20.22±3.27; *Figure 5D*).

Both engrafted CTRL-ASCs and ITGB2-ASCs expressed angiogenic cytokines such as VEGF, HGF, and IGF-1 (*Figure 5A-5C*), indicating that survived and engrafted ASCs secreted significant amounts of multiple angiogenic growth factors in vivo. The number of ASCs

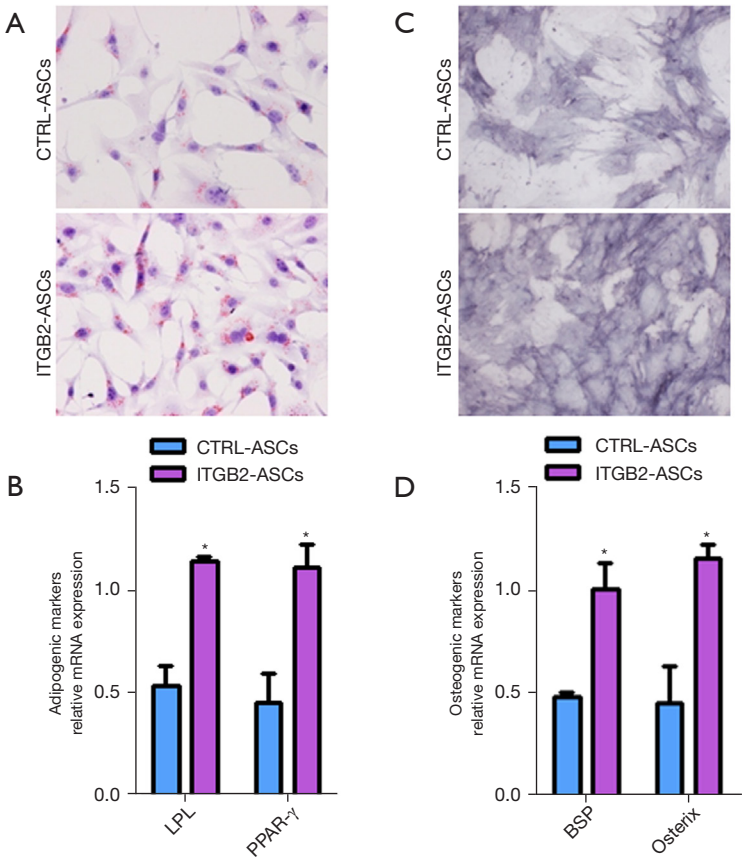

Figure 4 Enhancement of ASC-induced differentiation by ITGB2 overexpression *in vitro*. (A) Adipogenic differentiation was determined by staining with Oil Red O to visualize cytoplasmic lipid droplet accumulation. (B) ITGB2-ASCs displayed significantly higher levels of adipogenic-related genes LPL and PPAR-γ as compared to CTRL-ASCs. (C) Osteogenic differentiation was demonstrated by AP staining. (D) ITGB2-ASCs displayed significantly higher levels of osteogenic-related genes BSP and OSX when compared to CTRL-ASCs. Scale bar: 50 μm. *P<0.05 versus CTRL-ASCs. ASCs, adipose-derived stem cells; ITGB2, integrin β_2; CTRL, control; LPL, lipoprotein lipase; PPAR-γ, peroxisome proliferator-activated receptor gamma; AP, alkaline phosphatase; BSP, bone sialoprotein; OSX, osterix.

expressing angiogenic factors was significantly higher in the hearts that received ITGB2-ASCs implantation (21.72±8.04 cells per HPF) than in the hearts that underwent CTRL-ASCs treatment (10.45±3.19; *Figure 5E*).

ITGB2 overexpression of ASCs augmented angiogenesis in infarcted myocardium post-transplantation

Immunofluorescent detection of VWF, an endothelial marker, was used to identify the capillaries at 4 weeks after cell transplantation. VWF typically rises during the course of acute myocardial infraction and VWF secretion from endothelial cells is transiently elevated following acute myocardial infarction. The results indicated that capillary density was greater in the infarcted myocardium of rats treated with ITGB2-ASCs than in that of rats treated otherwise (*Figure 6A*). Capillary density was more increased in the hearts that received ITGB2-ASCs implantation (335.15±57.77 vessels/mm^2) than in the hearts that underwent CTRL-ASCs (255.80±49.52) or PBS control treatments (176.91±54.32; *Figure 6B*).

ITGB2 overexpression of ASCs improved blood flow in infarcted hearts post-transplantation

Figure 7A shows the representative 17-segment tomographic polar maps visualizing ^{13}N-NH_3·H_2O distribution and ^{13}N-NH_3·H_2O myocardial PET perfusion

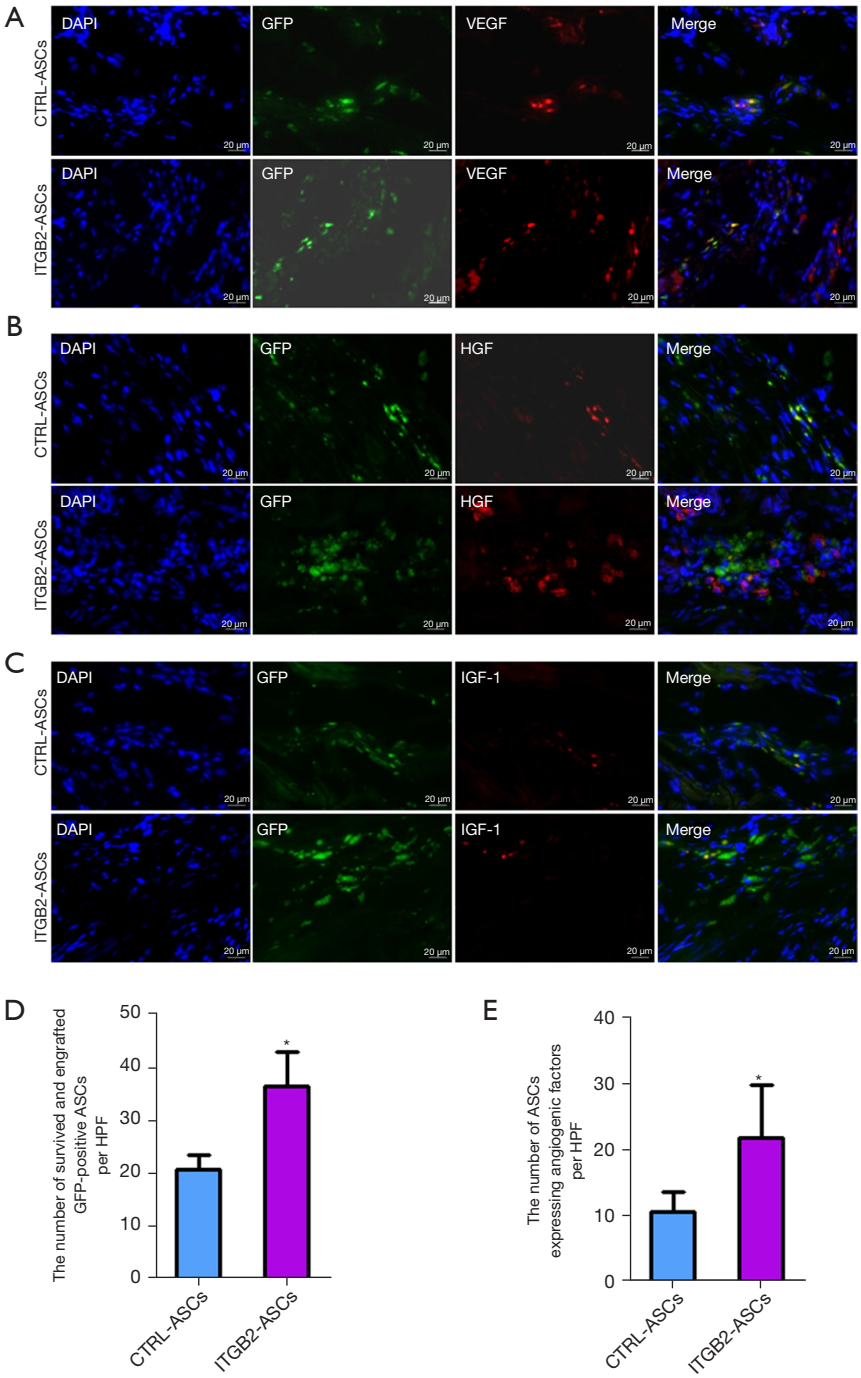

Figure 5 Enhancement of transplanted ASC engraftment by ITGB2 overexpression and angiogenic growth factors secreted by injected ASCs 4 weeks after transplantation in vivo. (A-C) Immunofluorescent staining was performed for angiogenic growth factors (red), and nuclei were stained with DAPI (blue). Both CTRL-ASCs and ITGB2-ASCs were identified by microscopic detection of GFP and secreted several angiogenic factors including VEGF, HGF, and IGF-1. (D) GFP-positive ASCs were more frequently engrafted into the ITGB2-ASC hearts when compared with the CTRL-ASC hearts. (E) ASCs expressing angiogenic growth factors were greater in the ITGB2-ASC hearts than in the CTRL-ASC hearts. Scale bar: 20 μm. *P<0.05 versus CTRL-ASCs. ASC, adipose-derived stem cells; ITGB2, integrin β_2; CTRL, control; GFP, green fluorescent protein; DAPI, 4, 6-diamidino-2-phenylindole; VEGF, vascular endothelial growth factor; HGF, hepatocyte growth factor; IGF-1, insulin-like growth factor-1; HPF, high power field.

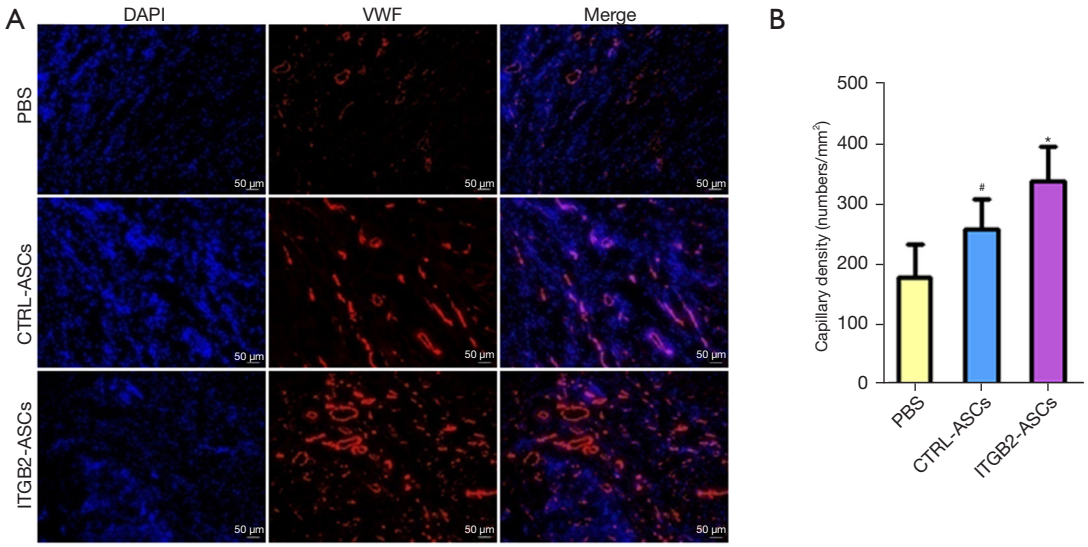

Figure 6 Enhancement of transplanted ASCs induced angiogenesis by ITGB2 overexpression 4 weeks after transplantation in vivo. (A) Immunofluorescent staining for VWF, an endothelial marker, was performed to identify capillaries. VWF-positive vessels were more frequently detected in the ITGB2-ASC hearts than in the CTRL-ASC hearts. (B) Capillary density was substantially greater in the ITGB2-ASC hearts than in the CTRL-ASC hearts and PBS control hearts. Scale bar: 50 μm. *P<0.05 versus CTRL-ASCs, #P<0.05 versus PBS. ASC, adipose-derived stem cells; ITGB2, integrin β_2; CTRL, control; DAPI, 4, 6-diamidino-2-phenylindole; VWF, Von Willebrand Factor; PBS, phosphate-buffered saline.

images of transverse, coronal, and sagittal planes at 4 weeks post-transplantation. Higher tracer uptake is visualized by the red and yellow colors and lower uptake by the green and blue colors. ^{13}N-NH_3·H_2O tracer uptake was obviously greater in infarcted hearts administered with ITGB2-ASCs than in those implanted with CTRL-ASCs or PBS control (*Figure 7A*). Standardized peak ^{13}N-NH_3·H_2O uptake of infarcted hearts were substantially greater in the ITGB2-ASC rats (63.94%±14.38%) than in the CTRL-ASC rats (53.61%±8.50%) and in the PBS control rats (43.76%±12.74%; *Figure 7B*).

Discussion

In this study, we genetically transfected ITGB2 into ASCs using a lentiviral-mediated infection technique and investigated the curative efficacy of ITGB2-ASCs on myocardial infarction. ICAM-1, a ligand of ITGB2, was substantially elevated at 3 days after myocardial infarction, remained upregulated 7 days after myocardial infarction, and attracted ITGB2-ASCs toward a gradient of ICAM-1. This suggested that ITGB2-ASCs have greater viability, faster proliferation, and stronger migration potential than CTRL-ASCs. In addition, our results suggested that ITGB2-ASCs engraft to ischemic myocardium more efficiently than CTRL-ASCs and contribute to the improvement of blood perfusion by inducing angiogenesis.

Integrins are cell surface transmembrane glycoproteins that function as adhesion receptors for ECM proteins and transfer the extracellular stimuli into intracellular biochemical signals. These signaling cascades regulate many cellular responses, such as survival, proliferation, migration, and spreading. Integrin-linked kinase (ILK) and focal adhesion kinase (FAK) are signaling proteins that are implicated in integrin signaling pathways. ILK improves MSC survival, enhances cell proliferation, and inhibits cell apoptosis, while ILK gene transduction of MSCs further assists cell survival and adhesion and improves myocardial damage when compared with control MSCs (27,28). Integrin-activated FAK interacts with a number of signaling and cytoskeletal proteins and regulates several integrin-mediated cellular events including the promotion of cell migration, proliferation, and spreading (29,30). *In vitro* results obtained from the present study showed that ITGB2-ASCs enhanced cell viability, proliferation, migration, and differentiation when compared to CTRL-ASCs. These results are consistent with prior reports indicating that ITGA5B1 enhances cell adhesion, cell

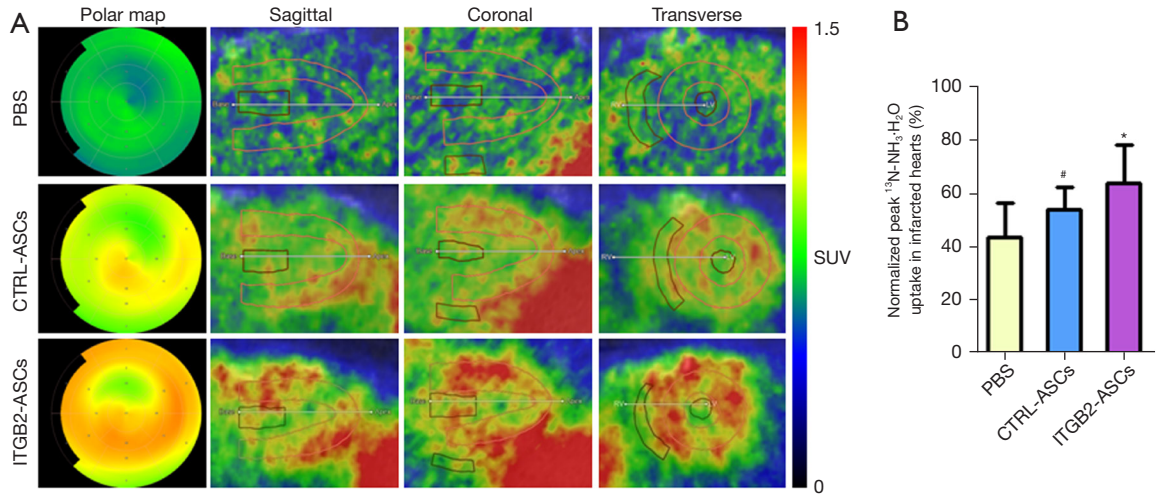

Figure 7 Enhancement of blood flow in infarcted hearts by ITGB2 overexpression of ASCs 4 weeks after transplantation *in vivo*. (A) Representative 17-segment polar map of the ^{13}N-NH$_3$·H$_2$O PET images and myocardial ^{13}N-NH$_3$·H$_2$O perfusion images at 4 weeks post-transplantation. Red and yellow colors were indicative of higher tracer uptake, while green and blue colors stood for lower tracer uptake. (B) Four weeks after transplantation, ITGB2-ASCs transplantation markedly elevated the peak ^{13}N-NH$_3$·H$_2$O uptake in infarcted hearts when compared with CTRL-ASCs and PBS control. *P<0.05 versus CTRL-ASCs, $^{\#}$P<0.05 versus PBS. ASC, adipose-derived stem cells; ITGB2, integrin β_2; CTRL, control; PET, positron emission tomography; PBS, phosphate-buffered saline; SUV, standard uptake value.

viability, cell migration and nitric oxide (NO) production but reduces cell apoptosis in BMSCs (31).

Integrins are involved in cell-to-cell and cell-to-ECM interaction. ICAM-1/ITGB2 binding plays a critical role in mediating the rolling of stem cells on the surface of endothelial cells, adhesion and transmigration through the vascular wall into interstitial tissue, and homing to ischemic tissue. The use of ligand–receptor interactions (ECM and integrins) are expected to improve the engraftment of transplanted ASCs. Our *in vivo* results demonstrated that ITGB2 overexpression enhances ASC survival and engraftment, indicating a more efficient interaction between ITGB2-ASCs and activated endothelium and subsequent transmigration. Our findings indicated that ITGB2 overexpression of ASCs augmented angiogenesis and improved blood flow in infarcted hearts. These results are in line with those of previous studies on ITG overexpression. The intravenous administration of endothelial colony-forming cells genetically modified to overexpress ITGB1 effectively stimulates angiogenesis in ischemic hindlimbs (32). Moreover, ITGB1 overexpression inhibits the apoptosis of transplanted BMSCs and contributes to enhanced cardiac repair after myocardial infarction (33).

Most of engrafted stem cells died within several days after grafting into infarcted hearts. Multiple mechanisms could contribute to the death of grafted stem cells, including hypoxic, nutrient deprivation, inflammatory environment after myocardial infarction, and loss of survival signal in cells (34). Recently, many kinds of methods have been developed to promote stem cell survival and engraftment into the infarcted heart, including optimal engrafting time, optimal culture conditions, transduced with survival-related genes, improving adhesion of transplanted stem cells, delivery methods, and preconditioning (34). The study found that the implantation of ASCs genetically modified to overexpress ITGB2 effectively stimulated angiogenesis and enhanced blood perfusion in infarcted function. ICAM-1, a ligand of ITGB2, is upregulated in infarcted myocardium. The interaction between extracellular matrix and integrins for homing represents substantial advantages distinct from previously reported strategies for improving the efficacy of stem cell.

Despite encouraging results, this study had several limitations. First, this intervention simultaneously involved stem cells and genetical modification, and preclinical safety studies on retrovirus vector-mediated gene therapy need to be conducted. Second, the therapy was administered at 3 days following myocardial ischemia. Clinically, patients might not arrive at the hospital for treatment within 3 days of experiencing a coronary ischemic insult. Third, the study

is largely an observation examination, and the detailed molecular mechanism by which ITGB2 enhances the biological activity of ASCs and promotes the engraftment of implanted ASCs was not further addressed in this study.

Conclusions

ASCs were lentivirally transduced to overexpress ITGB2. ICAM-1, a ligand of ITGB2, was significantly upregulated at 3–7 days after myocardial infarction. ITGB2 overexpression enhanced ASC viability, proliferation, and migration and induced differentiation in vitro. ITGB2 overexpression enhanced the homing and engraftment of transplanted ASCs to infarcted myocardium through ICAM-1/ITGB2 interactions, augmented angiogenesis, and improved myocardial perfusion. Therefore, ASCs represent a novel therapeutic strategy for myocardial infarction.

Acknowledgments

Funding: This work was supported by the National Natural Sciences Foundation of China (No. 81770277), the Natural Science Foundation of Hubei Province of China (No. 2015CFB457), the Key Laboratory of Biological Targeted Therapy of Hubei Province (No. 2021swbx020), and the Science Foundation of Wuhan Union Hospital (No. 2021xhyn109).

Footnote

Reporting Checklist: The authors have completed the ARRIVE reporting checklist. Available at https://atm.amegroups.com/article/view/10.21037/atm-22-3339/rc

Data Sharing Statement: Available at https://atm.amegroups.com/article/view/10.21037/atm-22-3339/dss

Conflicts of Interest: All authors have completed the ICMJE uniform disclosure form (available at https://atm.amegroups.com/article/view/10.21037/atm-22-3339/coif). The authors have no conflicts of interest to declare.

Ethical Statement: The authors are accountable for all aspects of the work in ensuring that questions related to the accuracy or integrity of any part of the work are appropriately investigated and resolved. Experiments were performed under a project license (No. 2017-392) granted by the Institutional Animal Ethical Committee (IAEC) of Huazhong University of Science and Technology, in compliance with institutional guidelines for the care and use of animals.

References

1. Sabol RA, Bowles AC, Côté A, et al. Therapeutic Potential of Adipose Stem Cells. Adv Exp Med Biol 2021;1341:15-25.
2. Khazaei S, Keshavarz G, Bozorgi A, et al. Adipose tissue-derived stem cells: a comparative review on isolation, culture, and differentiation methods. Cell Tissue Bank 2022;23:1-16.
3. Ning H, Liu G, Lin G, et al. Fibroblast growth factor 2 promotes endothelial differentiation of adipose tissue-derived stem cells. J Sex Med 2009;6:967-79.
4. Planat-Benard V, Silvestre JS, Cousin B, et al. Plasticity of human adipose lineage cells toward endothelial cells: physiological and therapeutic perspectives. Circulation 2004;109:656-63.
5. Rodríguez LV, Alfonso Z, Zhang R, et al. Clonogenic multipotent stem cells in human adipose tissue differentiate into functional smooth muscle cells. Proc Natl Acad Sci U S A 2006;103:12167-72.
6. Yogi A, Rukhlova M, Charlebois C, et al. Differentiation of Adipose-Derived Stem Cells into Vascular Smooth Muscle Cells for Tissue Engineering Applications. Biomedicines 2021;9:797.
7. Huang H, Tang X, Li S, et al. Advanced platelet-rich fibrin promotes the paracrine function and proliferation of adipose-derived stem cells and contributes to micro-autologous fat transplantation by modulating HIF-1α and VEGF. Ann Transl Med 2022;10:60.
8. Wang Y, Wang S, Gu C, et al. Ex-vivo treatment of allografts using adipose-derived stem cells induced prolonged rejection-free survival in an allogenic hind-limb transplantation model. Ann Transl Med 2020;8:867.

9. Bai X, Yan Y, Song YH, et al. Both cultured and freshly isolated adipose tissue-derived stem cells enhance cardiac function after acute myocardial infarction. Eur Heart J 2010;31:489-501.
10. Yasuda T, Weisel RD, Kiani C, et al. Quantitative analysis of survival of transplanted smooth muscle cells with real-time polymerase chain reaction. J Thorac Cardiovasc Surg 2005;129:904-11.
11. Moelker AD, Baks T, van den Bos EJ, et al. Reduction in infarct size, but no functional improvement after bone marrow cell administration in a porcine model of reperfused myocardial infarction. Eur Heart J 2006;27:3057-64.
12. Müller-Ehmsen J, Krausgrill B, Burst V, et al. Effective engraftment but poor mid-term persistence of mononuclear and mesenchymal bone marrow cells in acute and chronic rat myocardial infarction. J Mol Cell Cardiol 2006;41:876-84.
13. Zhang H, Chen H, Wang W, et al. Cell survival and redistribution after transplantation into damaged myocardium. J Cell Mol Med 2010;14:1078-82.
14. Hou D, Youssef EA, Brinton TJ, et al. Radiolabeled cell distribution after intramyocardial, intracoronary, and interstitial retrograde coronary venous delivery: implications for current clinical trials. Circulation 2005;112:I150-6.
15. Li SH, Lai TY, Sun Z, et al. Tracking cardiac engraftment and distribution of implanted bone marrow cells: Comparing intra-aortic, intravenous, and intramyocardial delivery. J Thorac Cardiovasc Surg 2009;137:1225-33.e1.
16. Wang J, Xiang B, Deng JX, et al. Hypoxia enhances the therapeutic potential of superparamagnetic iron oxide-labeled adipose-derived stem cells for myocardial infarction. J Huazhong Univ Sci Technolog Med Sci 2017;37:516-22.
17. Chi C, Wang F, Xiang B, et al. Adipose-derived stem cells from both visceral and subcutaneous fat deposits significantly improve contractile function of infarcted rat hearts. Cell Transplant 2015;24:2337-51.
18. Li J, Hu S, Cheng K. Engineering better stem cell therapies for treating heart diseases. Ann Transl Med 2020;8:569.
19. Wang J, Xiang B, Deng J, et al. Externally Applied Static Magnetic Field Enhances Cardiac Retention and Functional Benefit of Magnetically Iron-Labeled Adipose-Derived Stem Cells in Infarcted Hearts. Stem Cells Transl Med 2016;5:1380-93.
20. Mrugacz M, Bryl A, Falkowski M, et al. Integrins: An Important Link between Angiogenesis, Inflammation and Eye Diseases. Cells 2021;10:1703.
21. Wang L, Zheng F, Song R, et al. Integrins in the Regulation of Mesenchymal Stem Cell Differentiation by Mechanical Signals. Stem Cell Rev Rep 2022;18:126-41.
22. Shu C, Han S, Hu C, et al. Integrin β1 regulates proliferation, apoptosis, and migration of trophoblasts through activation of phosphoinositide 3 kinase/protein kinase B signaling. J Obstet Gynaecol Res 2021;47:2406-16.
23. Li B, Rong Q, Du Y, et al. Regulation of β1-integrin in autophagy and apoptosis of gastric epithelial cells infected with Helicobacter pylori. World J Microbiol Biotechnol 2021;38:12.
24. Yoon CH, Hur J, Oh IY, et al. Intercellular adhesion molecule-1 is upregulated in ischemic muscle, which mediates trafficking of endothelial progenitor cells. Arterioscler Thromb Vasc Biol 2006;26:1066-72.
25. Stillwell C, Wang F, Xiang B, et al. Adipose tissue houses different subtypes of stem cells. Can J Physiol Pharmacol 2012;90:1295-301.
26. Ip JE, Wu Y, Huang J, et al. Mesenchymal stem cells use integrin beta1 not CXC chemokine receptor 4 for myocardial migration and engraftment. Mol Biol Cell 2007;18:2873-82.
27. Ding L, Dong L, Chen X, et al. Increased expression of integrin-linked kinase attenuates left ventricular remodeling and improves cardiac function after myocardial infarction. Circulation 2009;120:764-73.
28. Mao Q, Lin C, Gao J, et al. Mesenchymal stem cells overexpressing integrin-linked kinase attenuate left ventricular remodeling and improve cardiac function after myocardial infarction. Mol Cell Biochem 2014;397:203-14.
29. Zhao X, Guan JL. Focal adhesion kinase and its signaling pathways in cell migration and angiogenesis. Adv Drug Deliv Rev 2011;63:610-5.
30. Cary LA, Guan JL. Focal adhesion kinase in integrin-mediated signaling. Front Biosci 1999;4:D102-13.
31. Chen HY, Pan L, Yang HL, et al. Integrin alpha5beta1 suppresses rBMSCs anoikis and promotes nitric oxide production. Biomed Pharmacother 2018;99:1-8.
32. Goto K, Takemura G, Takahashi T, et al. Intravenous Administration of Endothelial Colony-Forming Cells Overexpressing Integrin β1 Augments Angiogenesis in Ischemic Legs. Stem Cells Transl Med 2016;5:218-26.

33. Li L, Guan Q, Dai S, et al. Integrin β1 Increases Stem Cell Survival and Cardiac Function after Myocardial Infarction. Front Pharmacol 2017;8:135.
34. Shi RZ, Li QP. Improving outcome of transplanted mesenchymal stem cells for ischemic heart disease. Biochem Biophys Res Commun 2008;376:247-50.

(English Language Editor: C. Gourlay)

Cite this article as: Yuan Z, Yan K, Wang J. Overexpression of integrin β_2 improves migration and engraftment of adipose-derived stem cells and augments angiogenesis in myocardial infarction. Ann Transl Med 2022;10(16):863. doi: 10.21037/atm-22-3339

